

Key Points:

- The models of intra-crustal mantle imbrication beneath the Tibetan Plateau are critically discussed
- High-resolution geophysical images and derived models exclude intra-crustal mantle imbrication, and evidence Indian plate underthrusting
- Future modeling efforts should be based on high-quality data, and include a broader spectrum of processes and parameters

Correspondence to:

G. Hetényi,
gyorgy.hetenyi@unil.ch

Citation:

Hetényi, G., & Cattin, R. (2026). Comment on “Raising the roof of the world: Intra-crustal Asian mantle supports the Himalayan-Tibetan orogen” by Sternai et al. *Tectonics*, *45*, e2025TC009214. <https://doi.org/10.1029/2025TC009214>

Received 30 SEP 2025

Accepted 16 MAR 2026

Author Contributions:

Conceptualization: György Hetényi, Rodolphe Cattin

Data curation: György Hetényi

Formal analysis: György Hetényi

Investigation: György Hetényi, Rodolphe Cattin

Project administration: György Hetényi

Resources: György Hetényi, Rodolphe Cattin

Validation: György Hetényi, Rodolphe Cattin

Visualization: György Hetényi

Writing – original draft: György Hetényi

Writing – review & editing: György Hetényi, Rodolphe Cattin

Comment on “Raising the Roof of the World: Intra-Crustal Asian Mantle Supports the Himalayan-Tibetan Orogen” by Sternai et al.

György Hetényi¹  and Rodolphe Cattin² 

¹Institute of Earth Sciences, University of Lausanne, Lausanne, Switzerland, ²Géosciences Montpellier, University of Montpellier, Montpellier, France

Abstract The recent publication by Sternai et al. (2025, <https://doi.org/10.1029/2025tc009057>) presents numerical modeling results interpreted as—contrary to most publications over the past 100 years—it is Asian mantle imbricated between a thin Asian crust (above) and partially molten Indian crust (below) that characterizes the thickened structure of the Tibetan Plateau. We have serious concerns with both the structure and the geological time of the “Sternai” models. Most critically, Sternai et al. do not consider a wealth of high-resolution and high-quality geophysical (especially receiver-function and gravity) and geological data, which consistently characterize the lithosphere in the area as clearly showing Indian lower crust and mantle underthrusting the southern half of a thickened Tibetan crust. In this Comment, we detail our concerns and suggest that Sternai et al. carefully reconsider their models' input and output for a better understanding of the Himalaya-Tibet orogenic history.

1. Introduction

Sternai et al. (2025) performed 147 numerical thermodynamical model simulations of the Himalaya-Tibet orogen evolution, which “*systematically produced crustal doubling with interlayered mantle*” on the Asian side, based on—and compared with—selected geological and geophysical data. The authors emphasize that (i) their “*models focus on the Paleogene evolution of the India-Asia collision,*” and (ii) their “*main focus concerns the vertical juxtaposition of the Asian and Indian crusts by subduction, while other mechanisms of crustal thickening, for example, by upper plate crustal shortening, are beyond the primary purposes of their modeling.*”

We are most surprised by point (i) above, for the following reasons:

- If the model focus is on the Paleogene (66–23 Ma) evolution of the collision zone, then it is counterproductive to compare model results with geophysical images that reflect the current structure and properties of the orogen (see Section 2 below).
- On the contrary, if the actualistic geological and geophysical data are important *inputs* of the models as well as constraints on their results, then we find Sternai et al.'s data selection is highly incomplete and self-serving, as much better data sets with robust, consistent structure and features draw a drastically different picture of the orogen (see Section 3).

As we trust Sternai and co-authors' modeling expertise, we urge them to reconsider their modeling effort in light of a number of further thoughts summarized in Section 4. As developing new models may take time, we decided to write this formal Comment to draw the community's attention to the numerous problems with the models and interpretations by Sternai et al. (2025) and to not use them for the reasons detailed below. We emphasize that we do not contest the physics in the models but vividly contest the model setup and both the initial and boundary conditions, as well as the evaluation of the model results.

2. Paleogene Evolution—Model Time Does Not Correspond to Modern Observations

We agree with Sternai et al. that the collision of the India plate with the southern margin of Eurasia happened during the Paleogene (from ca. 66 to 23 Ma), and that the main process was subduction. If this time period is the main focus of their recent models, results should not be compared with geophysical images, as these images capture the current structure and physical properties of the lithosphere. Therefore, such comparisons neglect more than 20 Myr of Neogene evolution. Geophysical images and subsequent models of the orogen—presented below

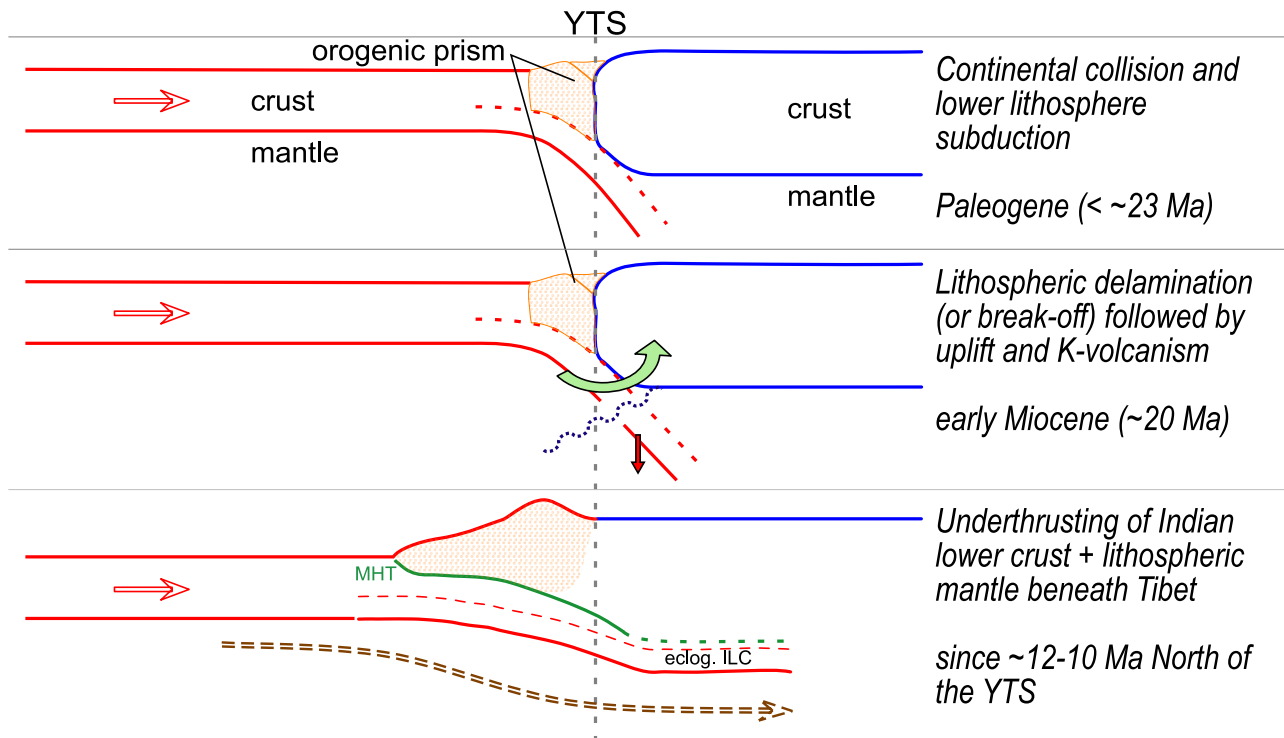


Figure 1. Schematic sketch of the collision of India (left, red) with the proto-Tibetan Plateau (right, blue) in three phases: subduction, followed by delamination/break-off, leading to the currently imaged structures showing underthrusting. Ages are approximate and are discussed in the main text. Abbreviations: MHT—Main Himalayan Thrust; ILC—Indian Lower Crust; YTS—Yarlung Tsangpo Suture.

in Section 3—robustly and consistently show that, along the central longitudes of Tibet, the prevailing process since at least 10 Myr is underthrusting of the Plateau from the south. This also implies that some time during the early Miocene a slab break-off or delamination event has happened (Figure 1). Modeling that process as a phase following subduction would be most useful, including the necking and detachment of a downgoing piece of (mantle) lithosphere, the position of which could be compared with seismic tomographic anomalies deeper in the mantle (Van der Voo et al., 1999, and subsequent works). In parallel, investigating what the fate of a possible Asian mantle imbrication is during the Neogene would be of interest: will the partially molten continental crust extrude southwards? Will it cause the foundering of the Plateau?

An important aspect of Paleogene models would be to consider the longer history of the Eurasian side of the collision, too. The Tibetan Plateau is the result of a series of four accreted terrains, each defining a tectonic block and a corresponding suture, from the lower Paleozoic to the late Jurassic (Tapponnier et al., 2001). As a result, the proto-plateau was already at an average altitude of ca. 2,000 m (Hu et al., 2020), reaching up to ca. 3,000 m in the Gangdese Mountains (Ding et al., 2022) prior to the collision with India, and therefore it already had a thickened crust. The modeling should therefore step away from a relatively thin, rather rigid crust and mantle lithosphere, as in the model setup of Sternai et al., and allow “other mechanisms of crustal thickening, for example, upper plate crustal shortening” (see point (ii) above) to happen. While the authors state this process is “beyond the primary purpose of their modeling,” the evolution of the Himalaya-Tibet orogen cannot be realistically simulated without allowing for such thickening to happen.

3. Comparison With Field Data—Structures Matter

Given the title of Sternai et al.'s paper and the close comparison of their model results with seismological and geological data, we believe that such structural elements, physical properties (esp. seismic velocities), and geological information were important inputs and constraints to their work. However, their choice of data was highly selective, partial (i.e., showing only a part of a profile) and incomplete (other types of data sets were not taken into account, e.g., gravity data). The choice of any author to consider only a few, suitably selected data

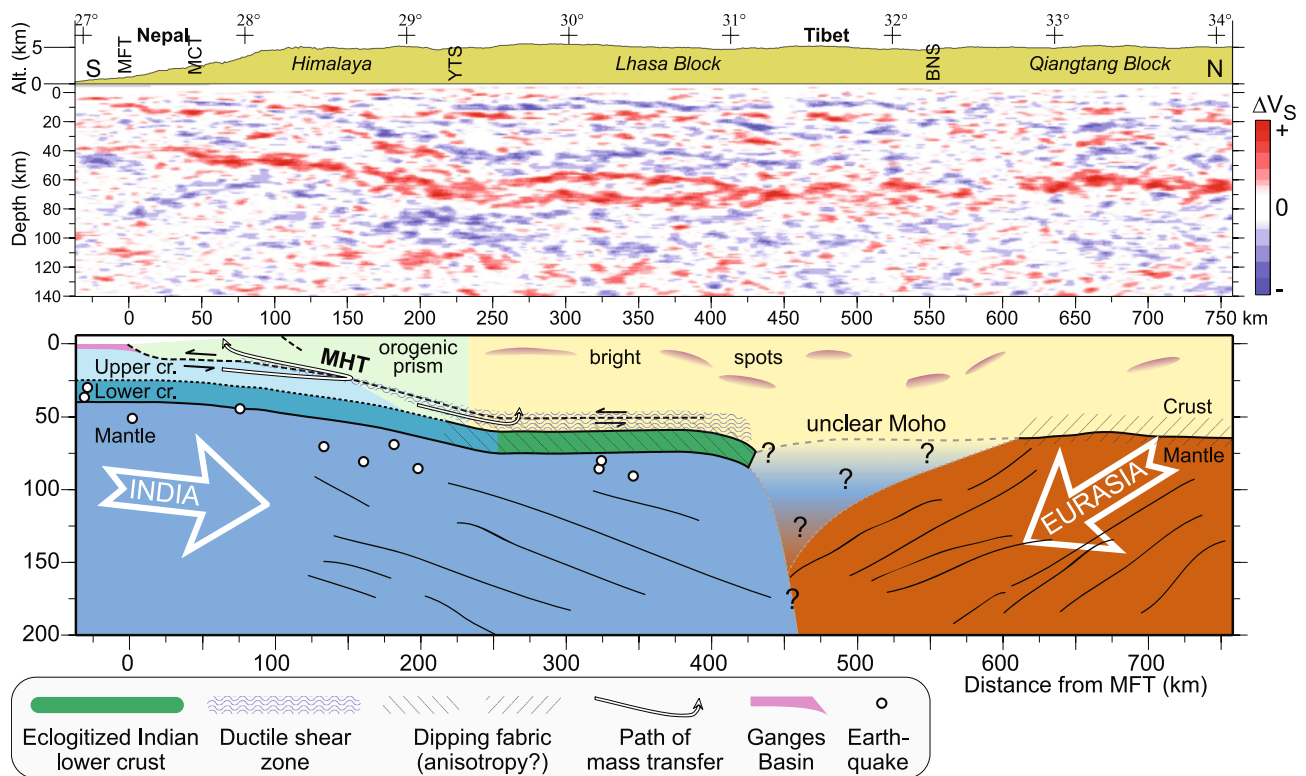


Figure 2. Composite receiver-function (direct and multiple conversions) image migrated to depth using a regional velocity model, and the corresponding lithospheric model of the Himalaya-Tibet collision along ca. 85°E. While the upper crust of the India plate feeds the orogenic prism, the lower crust and the mantle underthrust southern Tibet (Lhasa block) along the megathrust (Main Himalayan Thrust, MHT) and its continuation. Figures taken from Hetényi (2007); we refer to that work for full details. Abbreviations: MFT—Main Frontal Thrust; MCT—Main Central Thrust; YTS—Yarlung Tsangpo Suture; BNS—Banggong-Nujiang Suture.

points is not a validation of the model results. Before critically reviewing these elements, we first present the seismological image and joint models built upon that support the current view of crustal thickening in the Himalaya-Tibet region.

3.1. Underthrusting: Image and Consistent, Joint Modeling Results

The Hi-CLIMB seismological experiment's images provide the highest resolution and highest quality images across Himalaya-Tibet orogen. This is thanks to the experiment's densely spaced stations, long deployment time, and state-of-the-art processing using several converted waves (receiver-functions) (see e.g., Hetényi, 2007; J. Nábělek et al., 2009; Wittlinger et al., 2009). The images clearly reveal flexure of the Indian plate beneath the Himalaya, followed by sub-horizontal underthrusting beneath southern Tibet with a characteristic seismic “doublet”: two, sub-horizontal interfaces at ca. 15 km depth difference (Figure 2). A large number of other publications imaged both the sub-Himalayan downgoing part (e.g., Acton et al., 2011; Caldwell et al., 2013; Hauck et al., 1998; Rai et al., 2006; Schulte-Pelkum et al., 2005; Singer et al., 2017; Subedi et al., 2018) and the underthrusting part (e.g., Kind et al., 2002; Shi et al., 2015; Wittlinger, Farra, & Vergne, 2004; Wittlinger, Vergne, et al., 2004; Xu et al., 2015) at various longitudes of the orogen, thus providing strong evidence for this structural setup.

The imaged structures were the solid foundation to build two numerical models of the lithosphere that jointly fit several parameters. A thermodynamic model simulated the flexure of the India plate under the load of the Tibetan Plateau, in which the evolution of the rheological structure of the lithosphere shows decoupling of its main layers, and highlights that the primary support of the high topography is by the strong Indian mantle lithosphere (Cattin et al., 2001; Hetényi et al., 2006). A thermo-kinematic model, coupled with petrological and density modeling showed that the Indian lower crust is turning into eclogite beneath southern Tibet (Hetényi et al., 2007), explaining the seismic “doublet” seen by receiver-functions (Hetényi, 2007; J. Nábělek et al., 2009). Gravity anomalies acquired in the field constrained density distribution and allowed construction of joint models

including multiple physical properties to congruently show that the Indian lower crust underthrusts the southern Tibetan Plateau for >200 km distance north of the Yarlung Tsangpo Suture (YTS), the geological northern boundary of Indian rocks at the surface (Figure 2).

The geometry and convergence rate of this model also constrain the timing of the underthrusting. Considering 17 mm/yr underthrusting and 4 mm/yr overthrusting velocity across the Himalaya (Bollinger et al., 2006),—as the rest of the India-Eurasia convergence is accommodated further North,—the time to underthrust ca. 200 km distance north of the YTS (Figure 2) is 9.5–12 Myr. If the delamination/slab-breakoff occurred farther south than the YTS, the duration of underthrusting is longer, up to even 20 Myr. The transition from Paleogene subduction to break-off and to Neogene underthrusting (Figure 1) is therefore an interesting yet challenging target for numerical modeling.

Although the high-resolution image of underthrusting is in 2D, many other profiles with somewhat lower resolution also reveal the “doublet” (see references cited above) to be present laterally under the southern 450 km of the Himalaya-Tibet orogen with respect to the collision front (Hetényi, 2007; J. Nábělek et al., 2009). The lateral continuity of the Indian underthrusting is a question, as for example, J. Li and Song (2018) propose tearing, which could allow local upwelling from below, possibly influencing the formation of extensional rifts in southern Tibet (Armijo et al., 1986).

It is to this summary understanding of the Himalaya-Tibet orogen that we compare the models produced—and the data selected—by Sternai et al. (2025).

3.2. Critiques of Sternai et al. (2025) Data Selection and Models

3.2.1. Structural Seismology, Seismic Velocities, and Seismicity

3.2.1.1. Misinterpretation of the Composite Receiver-Function Image

Although Sternai et al. (2025) chose our migrated receiver-function image as a base for their study, their selection is partial (their Figure 1c does not show the full profile) and the interpretation drawn on the profile is erroneous (see below). As the selected seismological picture is a composite image of direct and multiple wave conversions, not every “blue” (negative) line corresponds to a velocity decrease with depth. We refer to Hetényi (2007) and J. Nábělek et al. (2009) for technical details of non-linear stacking of the various converted wave phases.

3.2.1.2. Incorrect Identification of Eclogitic Crust

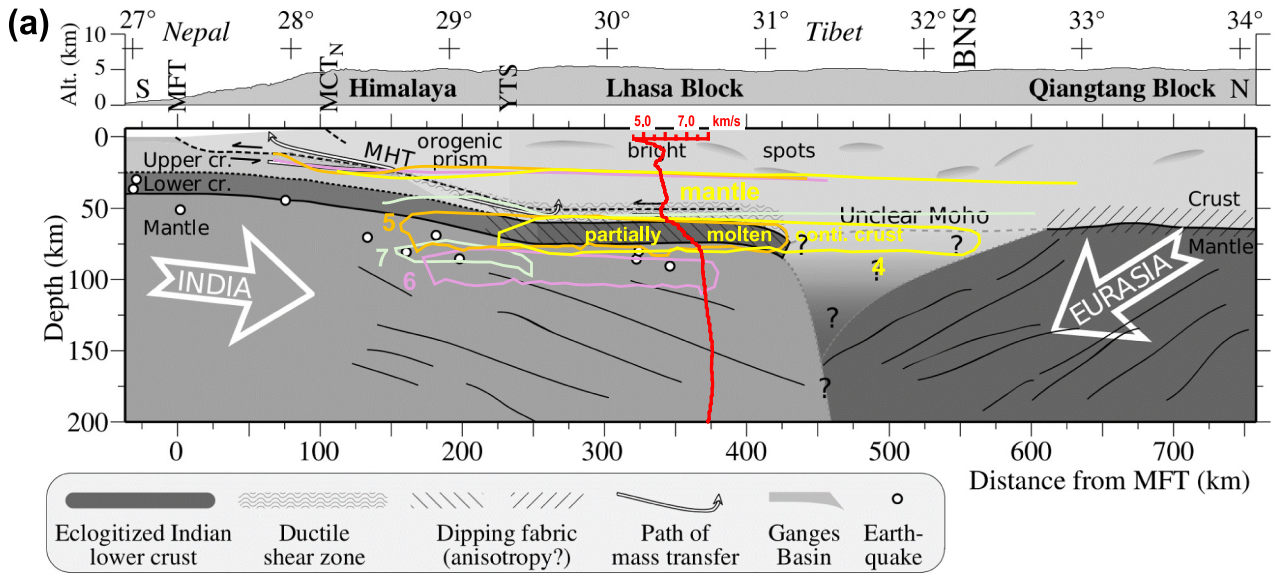
On the same image, Sternai et al.'s line drawing of “Indian eclogitic crust” continues the top of this layer southwards in what is actually the Moho (see our Figure 2). We emphasize that until about 200 km horizontal distance the main “red” (positive) interface is the Moho, and the seismic “doublet” further north appears because of eclogitization of the lower crust: the top interface is the crust-to-eclogite, and the bottom is the eclogite-to-mantle boundary. The modeled P-wave velocity of the eclogite layer is 7.5 km/s according to the coupled thermokinematic-petrological model mentioned above (see Hetényi, 2007; Hetényi et al., 2007). Thus, the receiver-function image clearly shows underthrusting, at depths between ~58 and ~73 km below sea-level beneath the Lhasa block, as detailed in Section 3.1.

3.2.1.3. Absence of an Imaged Shallow Asian Moho

The main feature of Sternai et al.'s model is the imbricated mantle on the Asian side of the collision. Three of the four models they present with figures feature an Asian Moho interface at 25 km depth below sea-level, and one model at ~55 km depth (see their figures 4-5-6-7, redrawn on our interpreted profile as Figure 3 of this paper). The Hi-CLIMB receiver-function images show no converted phase that could be associated with such a shallow Moho (see J. Nábělek et al., 2009, several images in Hetényi, 2007, and several local velocity-models in Hetényi et al., 2011). Therefore, the mantle imbrication obtained in Sternai et al.'s models is invalidated by current geophysical data. The reasons *why* a “shallow Moho” appears in the numerical models remain to be elucidated.

3.2.1.4. Mismatch of Selected Real Receiver-Functions and Synthetic Waveforms

Sternai et al. show a single synthetic receiver-function waveform in their figure 9c, and compare it to real-data receiver-functions at a single station, YS78 (from fig. 2c of Shi et al., 2020, not Shi et al., 2015, as cited by



Grayscale: Hetényi 2007 PhD Thesis, figure 5.17, later published in Nábělek et al. 2009 Science

Red: V_p profile from Nábělek et al. 2009 Science

Other contours (4, 5, 6, 7): Sternai et al. 2025 Tectonics

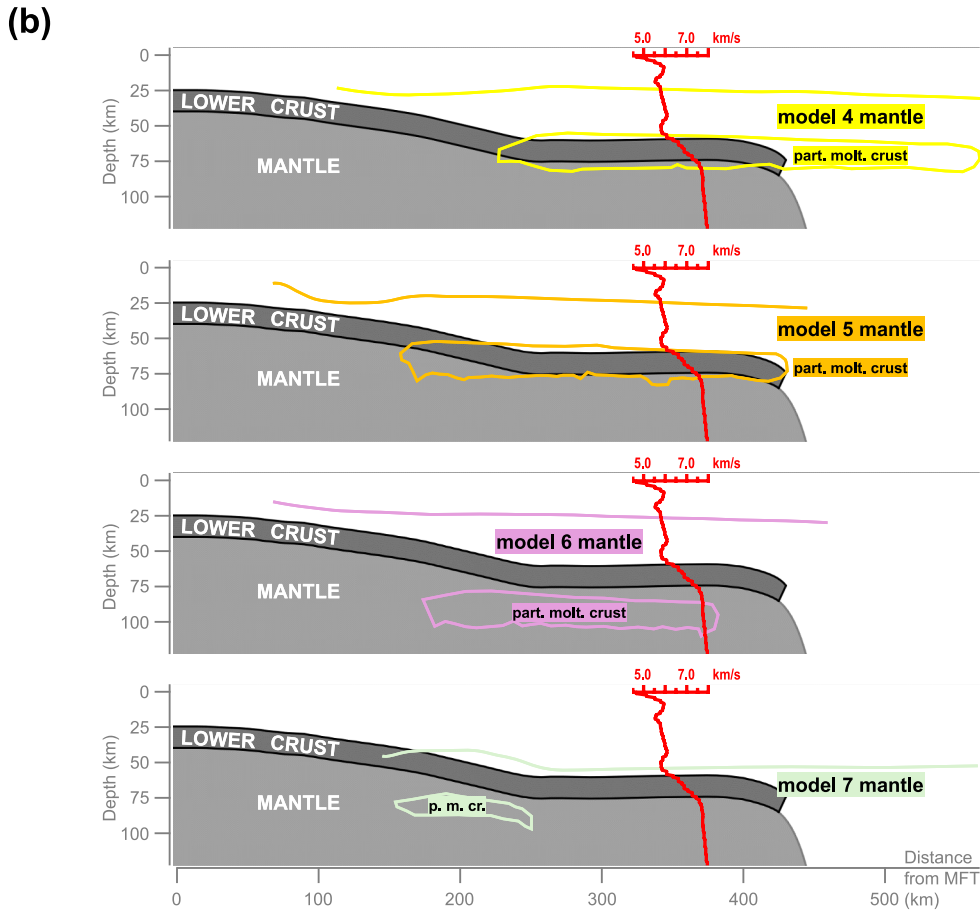


Figure 3.

Sternai et al.), out of 178 stations discussed in the cited paper. First, the seismic doublet appears at depths corresponding to eclogitized lower crust, while Sternai et al.'s synthetic receiver-function shows only a single peak and no doublet. Most importantly, the entire point of Shi et al. (2020) is that the receiver-functions map out systematic and important lateral variability of the near-Moho “doublet.” The single station that Sternai et al. chose and claimed to be “representative” in not showing the doublet is the unusual case, not the common case. Shi et al. (2020), in their same Fig. 2c, contrast YS78 with YS91 to the west and LM47 to the east. Neither of these other two stations remotely matches the Sternai' synthetic. The comparison shown by Sternai et al. is misleading; for such comparisons, in general, we would recommend fitting a larger set of real data.

3.2.1.5. Real Data Not Supporting Partially Molten Layer

Finally, a partially molten layer below the Asian mantle, as proposed by Sternai et al., would have a very different receiver-function signature compared to the data observed by Hi-CLIMB. If such a partially molten layer was present at the position where Sternai et al.'s models show, it would also be detectable by other seismological approaches at the regional scale. However, to our knowledge, such a feature has not been observed.

3.2.1.6. Crustal Velocity Model Mismatch

Sternai et al. show a single shear-wave velocity profile (from Galvé et al., 2002) to support their model of an imbricated Asian mantle. The seismological station at which this S-wave velocity profile was observed (station T in Galvé et al., 2002) is located South of the YTS, and is therefore not representative of the Lhasa block structure to the North of the YTS. Numerous other analyses exist for regional average 1D velocity models, already from the same time period (e.g., Haines et al., 2003, for average 1D models of Lhasa and Qiangtang blocks) and also later. From the Hi-CLIMB experiment, J. Nábělek et al. (2009) report a characteristic Lhasa block P-wave velocity profile, which we show in Figure 3: velocities throughout the Tibetan upper and middle crust are at ~ 6 km/s, without any increase at depths where Sternai et al.'s imbricated mantle lies. P-wave velocity increases in the underthrusting eclogite layer before reaching the mantle values, as also seen in Wang et al. (2021, their figure 2b). Such a regular crustal velocity model leaves no room for Asian mantle imbrication.

3.2.1.7. Tomographic Constraints

One of the inputs to Sternai et al.'s models was tomographic images that suggest Indian subduction at the southern margin of Tibet. We argue that the global tomographic images of C. Li et al. (2008) and Replumaz et al. (2004) are not sufficiently resolved to constrain regional features properly. When considering a relevant seismic velocity anomaly to identify a slab, these works do not demonstrate a continuous high-velocity anomaly from surface to depth at the YTS (e.g., profile III in Replumaz et al., 2004, with a color scale saturated at 0.8% anomaly). While their works would be very useful to match the longer geological history of subduction (the same as Van der Voo et al., 1999, see Section 2), we would recommend to use more recent and greatly improved full-waveform tomographies of Tibet (Dou et al., 2024; C. Liu et al., 2024; Ma et al., 2025) to set up and/or constrain numerical models.

3.2.1.8. Seismicity

Sternai et al. argue that the bimodal depth distribution of Tibetan seismicity is readily explained by the rigid, imbricated mantle that is able to support stresses, and that the “classical model of crustal doubling contradicts the observation of reduced seismicity from ~ 30 to 60 km depth.” Numerous studies have scrutinized seismicity in southern Tibet, concluding that shallow (upper crustal) seismicity is tectonic, the lack of seismicity in the Tibetan middle crust is due to elevated temperatures, and the deep crustal/mantle lithosphere seismicity is related to both

Figure 3. (a) Comparison of geophysically imaged and modeled structure (base image from Figure 2 in grayscale, Hetényi, 2007) versus numerically modeled layers (light color overlays from Sternai et al., 2025). The typical Lhasa Block P-wave velocity profile is shown in red (from J. Nábělek et al., 2009). Sternai et al.'s four main model geometries after 35–37 Ma simulation time are overlain in four light colors, using sea-level as horizontal reference and the position of their model's trench to match the MFT (Main Frontal Thrust, as the deepest point of the sedimentary basin). Yellow text labels indicate the layers in their reference model. See the main text for the critiques following this comparison. (b) Individual comparison of the main structures between those geophysically imaged structures, and each of the four models from Sternai et al. The abbreviation “p. m. cr.” refers to “partially molten continental crust.”

tectonic stresses and to metamorphic dehydration reactions during eclogitization. For details, we refer to Monsalve et al. (2006), Alvizuri and Hetényi (2019), Michailos et al. (2021) and references therein.

3.2.2. Thermal Structure

Another striking difference between Sternai et al.'s and our models is the temperature field. Our model-setup is based on Bollinger et al. (2006) who, using dense field observations across the Himalayan range in Central Nepal, have matched three different field observations while constraining the thermal state of the collision zone: inverse metamorphic gradients, peak temperatures, and exhumation ages. Our subsequent models reach ca. 700°C at depths characteristic of the Indian lower crust (Hetényi et al., 2007). Compared to this,—and also to most other models of the collision zone (e.g., Craig et al., 2012, 2020; Herman et al., 2010; P. I. Nábělek & Nábělek, 2014),—Sternai et al.'s models are much warmer, between 800 and 1000°C for the crust in their reference model and even higher in their other models. How well their model fits the dense field data from Bollinger et al. (2006) and subsequent studies is to be tested. In any case, the model temperatures would certainly change with other model setups and initial conditions. Importantly, the temperature changes will directly impact the rheological behavior of the lithospheric layers, therefore it is a key point to include among the parameters to fit by modeling.

3.2.3. Geological Data

There is a wealth of geological data from the Tibetan Plateau and the Himalaya, and it is not our goal here to provide an overview. We simply aim to point out that the data selected by Sternai et al. do not provide unique validity to their models—those data also fit our models.

In the Lhasa block, potassic volcanism appears to have been active between ~20–16 and ~10–8 Ma (C. Z. Liu et al., 2011; Turner et al., 1996). This activity fits well with our time evolution model, in which underthrusting follows delamination/break-off, as the time window (see above and Figure 1) coincides with the transition period during which there is no obstacle for potassic magmas to rise. As written in C. Z. Liu et al. (2011), a reference also cited by Sternai et al.: “*Indian underthrusting would have gradually shut off heat from the asthenosphere under the Lhasa terrane and terminated volcanism in southern Tibet.*”

Sternai et al. argue that the observation of helium isotope data ($^3\text{He}/^4\text{He}$ as a proxy for mantle) is challenging to reconcile with deep (>70 km) mantle sources, and their imbricated model is a more plausible source. However, considering the tears proposed by J. Li and Song (2018) and described above, we do not see any difficulty in sourcing helium from such depths to the surface via local upwellings through the tears. Moreover, their statement that “*It also seems unlikely that the plumbing system of geothermal springs can extend to >70 km depth*” may be true, but is certainly irrelevant: neither Klemperer et al. (2022) which they give the appearance of citing for this statement nor any other helium-worker makes this claim. Rather, the ductile lower crust is thought to be permeable to helium, which infiltrates the whole lower crust reaches faults in the brittle upper crust that supply active geothermal springs (e.g., Hilton, 2007). Unless Sternai et al. wish to similarly re-interpret the distribution of $^3\text{He}/^4\text{He}$ in the Andes, by intercalating a layer of mantle lithosphere beneath the volcanic arc and Altiplano in Earth's other area of over-thickened crust that is leaking mantle-enriched ^3He in its thermal springs, they may be advised to re-think their Tibetan model. Sternai et al. have a much bigger problem explaining the observed $^3\text{He}/^4\text{He}$ distribution in Tibet: their model shows “Asian mantle” continuing south of the YTS to reach the STD, and so predicts “mantle helium” being present south of the YTS to the STD. Klemperer et al. (2022) make it clear that the “mantle” ^3He -enriched domain is almost everywhere only north of the YZS. Thus, the claim by Sternai et al. that “*Interlayered mantle lithosphere at around ~50 km depth between underlying Indian and overlying Asian crust ... would readily explain the regional helium isotope data*” does not hold.

Various other geological data sets could and should be used in future models as constraints, such as the position of the YTS with respect to the collisional front, the structure of the Himalaya itself (Lower and Greater Himalayan Series), and the position and depth of origin of the granite and gneiss domes in southern Tibet, as examples.

3.2.4. Elevation Data

3.2.4.1. Paleoelevations Largely Differ From Model Elevations

Fitting the paleoelevations of the Tibetan Plateau must consider the uncertainty of the data itself, which is beyond the scope of this Comment. What is clear though is that Sternai et al. did not use this information to discriminate

the output of their models, which reproduce neither the paleo- nor the current elevations. In addition to the aforementioned question regarding the elevation of the proto-Tibetan Plateau, the elevation of -5 km of the Indian plain poses a problem. The obtained topography is unrealistic, with the relief between the Indian plain and the peaks of the Himalayas reaching more than 15 km at the end of the simulations (see their figures 5d, 6d, and 7d, and 12 km in their figure 4d). On the Tibet side, the elevation profiles after ca. 35 Ma model time are highly variable across the four models presented in their paper: about 2 km elevation of the reference model (their fig. 4d), a plateau starting at 4 km elevation for 200 km distance then tapering down to sea-level (their fig. 5d), an asymmetric plateau tapering from 5 to 0 km elevation in 300 km distance (their fig. 6d), and no plateau and near sea-level topography (their fig. 7d). In other words, the models do not “*raise the roof of the world*,” as the title of their paper claims.

3.2.4.2. Increase in Elevations in the Opposite Direction

Finally, contrary to the results of Sternai et al., “*with a progressive south-to-north uplift of Tibet driven by viscous underplating from the subduction interface toward the distal upper plate*,” paleoaltimetry data from the field suggest an increase in elevations spreading in the opposite direction, north-to-south from southern Qiangtang toward the Himalaya (Hu et al., 2020). This result is also confirmed by the compilation of Ding et al. (2022), which shows a rapid increase in elevation 40 and 20 Ma ago in the Lhasa-Qiangtang suture valley and southernmost Tibet, respectively. Once the focus on the model's time is clear, elevation data would be an important constraint on model results.

4. Toward Future Models of the Himalaya-Tibet Orogen

Despite the critiques expressed above, we hope that future modeling efforts by Sternai et al. and others in the community will be influenced by our Comment toward more realistic and data-driven models. While the amount of geological and geophysical data on the Himalaya-Tibet orogen is large, such future modeling efforts should select high-resolution, high-quality, and representative data sets based on original field data as their base and as evaluation criteria. For the model setup, this primarily concerns model structure (topography, thicknesses) and time evolution considerations for the initial conditions. For the assessment of model results, it seems crucial to attempt fitting multiple observations simultaneously.

The numerical modeling tool used by Sternai et al. is certainly robust and readily considers petrology and rheology. It should be able to produce outputs that can be compared to further, field-based constraints. Namely, for future modeling efforts, we suggest including the following:

- Gravity data, as it is an essential approach to distinguish density distributions within the lithosphere in an easily implementable way (see e.g., Bessat et al., 2020). Given the scale of the Tibetan Plateau's regional structure, the use of ground measurements is required, satellite data being able to resolve larger scale features (see Cattin et al., 2021, for the use of GOCE data in the area).
- The thermal field, using various field-based data sets and its implications for P-T conditions or ideally P-T-t evolution. For the Himalaya and Tibet, a wealth of data exists, the challenge is to fit multiple data sets simultaneously, as in for example, Bollinger et al. (2006).
- (Paleo-)Elevation data with a quantitative fit, including uncertainties (see Section 3.2.4). An essential element for future models will be adding surface processes, which will clearly impact the evolution of topography, foreland basin sedimentation and hence lithosphere dynamics.

Beyond multi-parameter or multi-field fits of model outputs, we believe that numerical models should encompass a broader range of parameter values for search. Without any intention to criticize Table 2 of Sternai et al. in particular, the range of variability is sometimes larger than initially assumed, partly because a complex 3D system is simplified into a 2D profile (excluding the use of seismic anisotropy as a constraint), and partly because of the temporal variability of rates. As an example, the significant portion of the collision that is accommodated by extrusion of Indochina is best modeled in 3D. Consequently, the shortening taken up by thickening or subduction in a 2D model is clearly less than in reality.

5. Conclusions

Our critiques of Sternai et al.'s models are motivated by the largely insufficient connection to original field data, primarily high-resolution seismology—the tool of choice for Earth structure imaging,—but also other elements such as gravity, elevation, and temperature, as well as their ambiguous choice of timing. We are fully convinced that no robust geophysical image or data set can support Asian mantle imbricated between Asian crust above and Indian crust below.

Our model among many others (Figure 2), based on high-quality data and models that jointly fit multiple parameters, clearly shows that the crust of southern Tibet is a thickened Asian crust (between ~5 km elevation and ~58 km depth below sea-level), underthrust by eclogitized Indian lower crust (~15 km thick, i.e., to 73 km depth) and Indian lithospheric mantle over 200 km distance north of the YTS. The high topography of Tibet and the Himalaya is mechanically supported by strong Indian mantle lithosphere.

Regarding modeling, we are of the opinion that inappropriately chosen model setup and initial conditions may have led to the unfortunate outcome of obtaining implausible model results reported by Sternai et al. Most importantly, future modeling efforts should focus on fitting multiple data sets simultaneously while respecting the original field data sets, together with covering a broader spectrum of processes—such as erosion and sedimentation—and parameters.

In summary, the discrepancies documented when comparing our high-quality geophysical and geological data and the consistent multi-parameter models built upon on one hand, versus the numerical simulation results presented by Sternai et al. on the other hand, suggest that the latter structures do not reflect a known orogenic model on Earth, and lead to misleading conclusions for future research. There is robust evidence that the primary process occurring at the central longitudes of the Himalaya-Tibet orogen is the underthrusting of the Indian lower crust and mantle lithosphere beneath southern Tibet—to first order, Argand (1924) was correct.

Conflict of Interest

The authors declare no conflicts of interest relevant to this study.

Availability Statement

All data shown and discussed in this document can be found in the cited references.

Acknowledgments

We greatly acknowledge all colleagues and persons—especially local people—involved in the field who enabled us and many other international, collaborative field experiments to collect the necessary data throughout the past decades in the Himalaya-Tibet area. We also thank several renowned Tibet- and Himalaya-specialist colleagues, who encouraged us to write this Comment, in particular Jérôme Lavé and Othmar Müntener, who provided useful input and feedback on the text within a brief time. We are grateful to Simon Klempner and Zhouchuan Huang for their very supportive and constructive reviews, as well as Taylor Schildgen and Giulio Viola for their editorial work.

References

- Acton, C. E., Priestley, K., Mitra, S., & Gaur, V. K. (2011). Crustal structure of the Darjeeling-Sikkim Himalaya and southern Tibet. *Geophysical Journal International*, 184(2), 829–852. <https://doi.org/10.1111/j.1365-246X.2010.04868.x>
- Alvizuri, C., & Hetényi, G. (2019). Source mechanism of a lower crust earthquake beneath the Himalayas and its possible relation to metamorphism. *Tectonophysics*, 769, 128153. <https://doi.org/10.1016/j.tecto.2019.06.023>
- Argand, E. (1924). La tectonique de l'Asie. In *Congrès Géologique Internationale, Bruxelles, Comptes rendus de la XIIIe session* (Vol. 1, pp. 171–372). Vaillant-Carmagne.
- Armijo, R., Tapponnier, P., Mercier, J. L., & Han, T. L. (1986). Quaternary extension in Southern Tibet—Field observations and tectonic implications. *Journal of Geophysical Research*, 91(B14), 13803–13872. <https://doi.org/10.1029/jb091ib14p13803>
- Bessat, A., Duretz, T., Hetényi, G., Pilet, S., & Schmalholz, S. M. (2020). Stress and deformation mechanisms at a subduction zone: Insights from 2D thermo-mechanical numerical modelling. *Geophysical Journal International*, 221(3), 1605–1625. <https://doi.org/10.1093/gji/ggaa092>
- Bollinger, L., Henry, P., & Avouac, J. P. (2006). Mountain building in the Nepal Himalaya: Thermal and kinematic model. *Earth and Planetary Science Letters*, 244(1–2), 58–71. <https://doi.org/10.1016/j.epsl.2006.01.045>
- Caldwell, W. B., Klempner, S. L., Lawrence, J. F., Rai, S. S., & Ashish (2013). Characterizing the Main Himalayan Thrust in the Garhwal Himalaya, India with receiver function CCP stacking. *Earth and Planetary Science Letters*, 367, 15–27. <https://doi.org/10.1016/j.epsl.2013.02.009>
- Cattin, R., Berthet, T., Hetényi, G., Saraswati, A., Panet, I., Cadio, C., et al. (2021). Joint inversion of ground gravity data and satellite gravity gradients between Nepal and Bhutan: New insights on structural and seismic segmentation of the Himalayan arc. *Physics and Chemistry of the Earth*, 123, 103002. <https://doi.org/10.1016/j.pce.2021.103002>
- Cattin, R., Martelet, G., Henry, P., Avouac, J. P., Diament, M., & Shukya, T. R. (2001). Gravity anomalies, crustal structure and thermo-mechanical support of the Himalaya of Central Nepal. *Geophysical Journal International*, 147(2), 381–392. <https://doi.org/10.1046/j.0956-540x.2001.01541.x>
- Craig, T. J., Kelemen, P. B., Hacker, B. R., & Copley, A. (2020). Reconciling geophysical and petrological estimates of the thermal structure of southern Tibet. *Geochemistry, Geophysics, Geosystems*, 21(8), e2019GC008837. <https://doi.org/10.1029/2019GC008837>
- Craig, T. J., Copley, A., & Jackson, J. (2012). Thermal and tectonic consequences of India underthrusting Tibet. *Earth and Planetary Science Letters*, 353–354, 231–239. <https://doi.org/10.1016/j.epsl.2012.07.010>
- Ding, L., Kapp, P., Cai, F., Garzzone, C. N., Xiong, Z., Wang, H., & Wang, C. (2022). Timing and mechanisms of Tibetan Plateau uplift. *Nature Reviews Earth & Environment*, 3(10), 652–667. <https://doi.org/10.1038/s43017-022-00318-4>

- Dou, H., Xu, Y., Lebedev, S., de Melo, B. C., van der Hilst, R. D., Wang, B., & Wang, W. (2024). The upper mantle beneath Asia from seismic tomography, with inferences for the mechanisms of tectonics, seismicity, and magmatism. *Earth-Science Reviews*, 255, 104841. <https://doi.org/10.1016/j.earscirev.2024.104841>
- Galvé, A., Sapin, M., Hirn, A., Diaz, J., Lépine, J., Laigle, M., et al. (2002). Complex images of Moho and variation of Vp/Vs across the Himalaya and South Tibet, from a joint receiver-function and wide-angle- reflection approach. *Geophysical Research Letters*, 29(24), 2182. <https://doi.org/10.1029/2002gl015611>
- Haines, S. S., Klemperer, S. L., Brown, L., Jingru, G. R., Mechie, J., Meissner, R., et al. (2003). INDEPTH III seismic data: From surface observations to deep crustal processes in Tibet. *Tectonics*, 22(1), 1001. <https://doi.org/10.1029/2001tc001305>
- Hauck, M. L., Nelson, K. D., Brown, L. D., Zhao, W., & Ross, A. R. (1998). Crustal structure of the Himalayan orogen at ~90° east longitude from Project INDEPTH deep reflection profiles. *Tectonics*, 17(4), 481–500. <https://doi.org/10.1029/98TC01314>
- Herman, F., Copeland, P., Avouac, J. P., Bollinger, L., Mahéo, G., Le Fort, P., et al. (2010). Exhumation, crustal deformation, and thermal structure of the Nepal Himalaya derived from the inversion of thermochronological and thermobarometric data and modeling of the topography. *Journal of Geophysical Research*, 115(B6), B06407. <https://doi.org/10.1029/2008jb006126>
- Hetényi, G. (2007). *Evolution of deformation of the Himalayan prism: From imaging to modelling* (Doctoral dissertation). École Normale Supérieure—Université Paris-Sud XI. Retrieved from <https://theses.hal.science/tel-00194619/en/>
- Hetényi, G., Cattin, R., Brunet, F., Vergne, J., Bollinger, L., Nábělek, J. L., & Diament, M. (2007). Density distribution of the India plate beneath the Tibetan Plateau: Geophysical and petrological constraints on the kinetics of lower-crustal eclogitization. *Earth and Planetary Science Letters*, 264(1–2), 226–244. <https://doi.org/10.1016/j.epsl.2007.09.036>
- Hetényi, G., Cattin, R., Vergne, J., & Nábělek, J. L. (2006). The effective elastic thickness of the India Plate from receiver function imaging, gravity anomalies and thermomechanical modelling. *Geophysical Journal International*, 167(3), 1106–1118. <https://doi.org/10.1111/j.1365-246X.2006.03198.x>
- Hetényi, G., Vergne, J., Bollinger, L., & Cattin, R. (2011). Discontinuous low-velocity zones in southern Tibet question the viability of the channel flow model. In R. Gloaguen & L. Ratschbacher (Eds.), *Growth and collapse of the Tibetan Plateau* (Vol. 353, pp. 99–108). Geological Society, London, Special Publications. <https://doi.org/10.1144/SP353.6>
- Hilton, D. R. (2007). The leaking mantle. *Science*, 318(5855), 1389–1390. <https://doi.org/10.1126/science.1151983>
- Hu, F., Wu, F., Chapman, J. B., Ducea, M. N., Ji, W., & Liu, S. (2020). Quantitatively tracking the elevation of the Tibetan Plateau since the cretaceous: Insights from whole-rock Sr/Y and La/Yb ratios. *Geophysical Research Letters*, 47(15), e2020GL089202. <https://doi.org/10.1029/2020GL089202>
- Kind, R., Yuan, X., Saul, J., Nelson, D., Sobolev, S. V., Mechie, J., et al. (2002). Seismic images of crust and upper mantle beneath Tibet: Evidence for Eurasian plate subduction. *Science*, 298(5596), 1219–1221. <https://doi.org/10.1126/science.1078115>
- Klemperer, S., Zhao, P., Whyte, C. J., Darrah, T. H., Crossey, L. J., Karlstrom, K. E., et al. (2022). Limited underthrusting of India below Tibet: ³He/⁴He analysis of thermal springs locates the mantle suture in continental collision. *Proceedings of the National Academy of Sciences*, 119(12), e2113877119. <https://doi.org/10.1073/pnas.2113877119>
- Li, C., van der Hilst, R., Engdahl, E. R., & Burdick, S. (2008). A new global model for P wave speed variations in Earth's mantle. *Geochemistry, Geophysics, Geosystems*, 9(5), Q05018. <https://doi.org/10.1029/2007gc001806>
- Li, J., & Song, X. (2018). Tearing of Indian mantle lithosphere from high-resolution seismic images and its implications for lithosphere coupling in southern Tibet. *Proceedings of the National Academy of Sciences*, 115(33), 8296–8300. <https://doi.org/10.1073/pnas.1717258115>
- Liu, C., Banerjee, R., Grand, S. P., Sandvol, E., Mitra, S., Liang, X., & Wei, S. (2024). A high-resolution seismic velocity model for East Asia using full-waveform tomography: Constraints on India-Asia collisional tectonics. *Earth and Planetary Science Letters*, 639, 118764. <https://doi.org/10.1016/j.epsl.2024.118764>
- Liu, C. Z., Wu, F. Y., Chung, S. L., & Zhao, Z. D. (2011). Fragments of hot and metasomatized mantle lithosphere in Middle Miocene ultrapotassic lavas, southern Tibet. *Geology*, 39(10), 923–926. <https://doi.org/10.1130/g32172.1>
- Ma, J., Song, X., Bunge, H.-P., Fichtner, A., & Tian, Y. (2025). Wholesale flat subduction of the Indian slab and northward mantle convective flow: Plateau growth and driving force of the India–Asia collision. *Proceedings of the National Academy of Sciences*, 122(7), e2411776122. <https://doi.org/10.1073/pnas.2411776122>
- Michailos, K., Carpenter, S. N., & Hetényi, G. (2021). Spatio-temporal evolution of intermediate-depth seismicity beneath the Himalayas: Implications for metamorphism and tectonics. *Frontiers in Earth Science*, 9, 742700. <https://doi.org/10.3389/feart.2021.742700>
- Monsalve, G., Sheehan, A., Schulte-Pelkum, V., Rajaure, S., Pandey, M. R., & Wu, F. (2006). Seismicity and one-dimensional velocity structure of the Himalayan collision zone: Earthquakes in the crust and upper mantle. *Journal of Geophysical Research*, 111(B10), B10301. <https://doi.org/10.1029/2005JB004062>
- Nábělek, J., Hetényi, G., Vergne, J., Sapkota, S., Kafle, B., Jiang, M., et al. (2009). Underplating in the Himalaya-Tibet collision zone revealed by the Hi-CLIMB experiment. *Science*, 325(5946), 1371–1374. <https://doi.org/10.1126/science.1167719>
- Nábělek, P. I., & Nábělek, J. L. (2014). Thermal characteristics of the Main Himalaya Thrust and the Indian lower crust with implications for crustal rheology and partial melting in the Himalaya orogen. *Earth and Planetary Science Letters*, 395, 116–123. <https://doi.org/10.1016/j.epsl.2014.03.026>
- Rai, S. S., Priestley, K., Gaur, V. K., Mitra, S., Singh, M. P., & Searle, M. (2006). Configuration of the Indian Moho beneath the NW Himalaya and Ladakh. *Geophysical Research Letters*, 33(15), L15308. <https://doi.org/10.1029/2006GL026076>
- Replumaz, A., Káráson, H., van der Hilst, R. D., Besse, J., & Tapponnier, P. (2004). 4-D evolution of SE Asia's mantle from geological reconstructions and seismic tomography. *Earth and Planetary Science Letters*, 221(1–4), 103–115. [https://doi.org/10.1016/s0012-821x\(04\)00070-6](https://doi.org/10.1016/s0012-821x(04)00070-6)
- Schulte-Pelkum, V., Monsalve, G., Sheehan, A., Pandey, M. R., Sapkota, S., Bilham, R., & Wu, F. (2005). Imaging the Indian subcontinent beneath the Himalaya. *Nature*, 435(7046), 1222–1225. <https://doi.org/10.1038/nature03678>
- Shi, D., Klemperer, S. L., Shi, J., Wu, Z., & Zhao, W. (2020). Localized foundering of Indian lower crust in the India–Tibet collision zone. *Proceedings of the National Academy of Sciences*, 117(40), 24742–24747. <https://doi.org/10.1073/pnas.2000015117>
- Shi, D., Wu, Z., Klemperer, S. L., Zhao, W., Xue, G., & Su, H. (2015). Receiver function imaging of crustal suture, steep subduction, and mantle wedge in the eastern India–Tibet continental collision zone. *Earth and Planetary Science Letters*, 414, 6–15. <https://doi.org/10.1016/j.epsl.2014.12.055>
- Singer, J., Kissling, E., Diehl, T., & Hetényi, G. (2017). The underthrusting Indian crust and its role in collision dynamics of the Eastern Himalaya in Bhutan: Insights from receiver function imaging. *Journal of Geophysical Research: Solid Earth*, 122(2), 1152–1178. <https://doi.org/10.1002/2016JB013337>
- Sternai, P., Pilia, S., Ghelichkhan, S., Bouilhol, P., Menant, A., Davies, D. R., et al. (2025). Raising the roof of the world: Intra-crustal Asian mantle supports the Himalayan-Tibetan orogen. *Tectonics*, 44(9), e2025TC009057. <https://doi.org/10.1029/2025TC009057>

- Subedi, S., Hetényi, G., Vergne, J., Bollinger, L., Lyon-Caen, H., Farra, V., et al. (2018). Imaging the Moho and the Main Himalayan Thrust in Western Nepal with receiver functions. *Geophysical Research Letters*, *45*(24), 13222–13230. <https://doi.org/10.1029/2018GL080911>
- Tapponnier, P., Xu, Z. Q., Roger, F., Meyer, B., Arnaud, N., Wittlinger, G., & Yang, J. S. (2001). Oblique stepwise rise and growth of the Tibet plateau. *Science*, *294*(5547), 1671–1677. <https://doi.org/10.1126/science.105978>
- Turner, S., Arnaud, N., Liu, J., Rogers, N., Hawkesworth, C., Harris, N., et al. (1996). Post-collision, shoshonitic volcanism on the Tibetan plateau: Implications for convective thinning of the lithosphere and the source of ocean island basalts. *Journal of Petrology*, *37*(1), 45–71. <https://doi.org/10.1093/petrology/37.1.45>
- Van der Voo, R., Spakman, W., & Bijwaard, H. (1999). Tethyan subducted slabs under India. *Earth and Planetary Science Letters*, *171*(1), 7–20. [https://doi.org/10.1016/s0012-821x\(99\)00131-4](https://doi.org/10.1016/s0012-821x(99)00131-4)
- Wang, G., Thybo, H., & Artemieva, I. M. (2021). No mafic later in 80 km thick Tibetan crust. *Nature Communications*, *12*(1), 1069. <https://doi.org/10.1038/s41467-021-21420-z>
- Wittlinger, G., Farra, V., Hetényi, G., Vergne, J., & Nábělek, J. (2009). Seismic velocities in Southern Tibet lower crust. A receiver function approach for eclogite detection. *Geophysical Journal International*, *177*(3), 1037–1049. <https://doi.org/10.1111/j.1365-246X.2008.04084.x>
- Wittlinger, G., Farra, V., & Vergne, J. (2004). Lithospheric and upper mantle stratifications beneath Tibet: New insights from Sp conversions. *Geophysical Research Letters*, *31*(19), L19615. <https://doi.org/10.1029/2004gl020955>
- Wittlinger, G., Vergne, J., Tapponnier, P., Farra, V., Poupinet, G., Jiang, M., et al. (2004). Teleseismic imaging of subducting lithosphere and Moho offsets beneath western Tibet. *Earth and Planetary Science Letters*, *221*(1–4), 117–130. [https://doi.org/10.1016/s0012-821x\(03\)00723-4](https://doi.org/10.1016/s0012-821x(03)00723-4)
- Xu, Q., Zhao, J., Yuan, X., Liu, H., & Pei, S. (2015). Mapping crustal structure beneath southern Tibet: Seismic evidence for continental crustal underthrusting. *Gondwana Research*, *27*(4), 1487–1493. <https://doi.org/10.1016/j.gr.2014.01.006>